JCTC Journal of Chemical Theory and Computation

ARTICLE

pubs.acs.org/JCTC

^1L_a and ^1L_b States of Indole and Azaindole: Is Density Functional Theory Inadequate?

Sundaram Arulmozhiraja* and Michelle L. Coote*

ARC Centre of Excellence for Free- Radical Chemistry and Biotechnology, Research School of Chemistry, Australian National University, Canberra, 0200 ACT, Australia

Supporting Information

ABSTRACT: The applicability of time-dependent density functional theory (TD-DFT) is tested in describing ^1L_a and ^1L_b $\pi-\pi^*$ states in indole, azaindole, indene, and benzimidazole. Several density functionals including popular three hybrid functionals (B3LYP, PBE0, and mPW1PW91), two meta-GGA functionals (M06-L and M06-2X), and four long-range corrected (CAM-B3LYP, ωB97XD, LC-BLYP, and LC-ωPBE) density functionals have been considered for the present study. The 6-311+G(2*d*,*p*) basis set incorporated with two sets of Rydberg *sp* functions for carbon and nitrogen atoms is utilized. The range-separation parameters for the calculations with the long-range corrected density functionals were tuned by enforcing the DFT version of Koopmans' theorem, and the effect of this tuning on the accuracy of the results is also examined. Results show that all of the hybrid and meta-GGA functionals predict a wrong order of ^1L_a and ^1L_b $\pi-\pi^*$ states in indole and azaindole. Although all of the LC functionals correctly predict that ^1L_b is the lowest excited state in indole, the energy gap calculated between the ^1L_b and ^1L_a state is much smaller than the value observed in the experimental studies. In the case of azaindole, only LC-ωPBE and LC-BLYP functionals could manage to reproduce the correct order of states; however, here too, the calculated energy gap between the two $\pi-\pi^*$ states is very small compared to the experimental value. Overall, the ^1L_b state excitation energies derived with all of the functionals are overestimated. In contrast, all of the nine selected functionals correctly reproduce the order of states in indene and benzimidazole. The origin of this differing performance is analyzed. Also in the study, oscillator strengths and dipole moments of the excited states are derived, and two other important states, $\pi-\sigma^*$ and $n-\pi^*$ states, that could play important role in the photochemistry of these molecules are examined.

1. INTRODUCTION

The indole chromophore is responsible for the low-energy absorption band of tryptophan.[1] Tryptophan fluorescence has become an important indicator of the protein environment and structural changes, primarily because the fluorescence spectrum and quantum yield of the indole chromophore are highly sensitive to its local microenvironment.[2−5] 7-Azatryptophan is one of the most successful alternative probes of protein structure and dynamics.[6] Hence, the excited states of indole and 7-azaindole, the chromophore of 7-azatryptophan, have attracted much attention in the context of understanding the complex photophysical behavior of tryptophanyl side chains of proteins.[7−20]

Azaindole is isoelectronic with purine and exhibits a close relationship with the nucleobases adenine and guanine. Thus, the azaindole dimer shows structural similarities to the adenine−thymine (A−T) and guanine−cytosine (G−C) base pairs of DNA. Investigations of excited state proton transfer reactions in the azaindole dimer may provide information about mutations of DNA induced by UV irradiation. Kasha and co-workers first studied the 7-azaindole dimer and provided a model for hydrogen bonding in DNA base pairs.[21] Since the doubly hydrogen-bonded dimer of 7-azaindole is a prototypical system that showed important excited-state double-proton transfer (ESDPT) character, its photochemistry and photophysics have been extensively studied. However, the question of whether proton transfer in the 7-azaindole dimer is a concerted or a stepwise mechanism remains in debate.[21−26]

An important step for understanding the photophysical behavior of these molecules is to understand the nature and the position of their low-lying electronic states. The low-energy absorption spectrum of these biologically important molecules is mainly characterized by two low-lying nearly degenerate $\pi-\pi^*$ excited states, the so-called ^1L_a and ^1L_b states, according to Platt nomenclature,[27] with different dipole moments that will determine the relative position of these two states as a function of the environment. The ^1L_b has a small dipole moment and gives rise to a structured band. The ^1L_a state produces a broad band, and its large dipole moment makes it sensitive to polar environments. It has been established that the ^1L_b state is the lowest excited singlet state in vapor-phase absorption spectra, the gas phase, and in nonpolar solvents, while the ^1L_a state becomes the lowest-energy (adiabatically) singlet state in polar solvents.[28−31]

Considering their significant biological roles and their use as optical probes in the study of proteins, an understanding of their electronic transitions and their spectral behavior becomes essential. *Ab initio* calculations have been used in the past to study the ^1L_a and ^1L_b states in indole and azaindole (by which we refer to the 7-azaindole for simplicity).[8,10−12,15,18,32] However, it is not always feasible to utilize high-level *ab initio* calculations to study large systems (such as the indole/azaindole derivatives and their dimers), and hence the identification of a reliable low-cost methodology

Received: October 31, 2011
Published: December 21, 2011

is also important. Time-dependent density functional theory (TD-DFT),[33−36] which is well-known for providing reliable valence excitation energies,[37−39] becomes the natural choice of alternative methodology for this purpose. However, it is known now that the conventional TD-DFT methods overstabilize charge-transfer[40−44] and Rydberg states.[45,46] Of particular importance is the work of Grimme and Parac,[47,48] who in 2003, showed that conventional TD-DFT methods fail to correctly describe the ^1L_a states in linear and nonlinear polycyclic aromatic hydrocarbons (PAHs). As a result, in many cases, these methods are unable to predict the relative order of the two low-lying states, ^1L_b and ^1L_a, correctly. It has been assumed that some sort of charge separation in the ^1L_a state was the reason for the errors observed in TD-DFT excitation energies for the ^1L_a state.[47] Nevertheless, DFT and TD-DFT methods with the popular B3LYP functional have been used to study the important excited-state double-proton transfer mechanism in the azaindole dimer.[49−53]

In recent years, long-range corrected (LC) functionals, which treat the electron−electron exchange interaction using HF at large separation and using GGA exchange at short-range, have been shown to work well for demanding charge transfer (CT) states,[54−56] including the challenging ^1L_a states of the linear acenes and of the nonlinear PAHs.[57,58] A recent study showed that LC-TDDFT (LC-BLYP) predicts an excited-state double-proton transfer mechanism in the azaindole dimer which is consistent with the more accurate CASPT2 results[59] but quite different from that predicted by conventional TD-DFT methods. However, although LC functionals generally provide better performance than conventional functionals for CT-like ^1L_a states in linear acenes and PAHs, the ^1L_b states in the same systems were not computed accurately.[57,58]

It has been shown in earlier studies that the results obtained using LC functionals are strongly influenced by the range-separation parameter (ω) that determines the balance of DFT and Hartree−Fock exchange at intermediate interelectronic distance r_{12}.[45,60−64] In most implementations, ω is adjusted in order to minimize average errors in geometries, atomization energies, barrier heights, ionization potentials, and other ground-state properties of a test set of molecules and treated as a universal constant for subsequent calculations. The optimal value differs for the properties of interest as well as for specific systems being studied,[63,64] and hence, one of the serious issues is the choice of the range-separation parameter.

Very recently, the Baer group and Kronik group have shown that the full predictive power of LC functionals can be obtained by optimally tuning the range-separation parameter using the first principle methods.[65−68] Their proposed tuning procedure is based on the requirement that in exact Kohn−Sham theory, the negative of the energy of the highest occupied molecular orbital (HOMO) is equal to its ionization potential (IP^N).

$$-{E_{\mathrm{HOMO}}}^N = \mathrm{IP} = E^{N-1} - E^N \quad (1)$$

where ${E_{\mathrm{HOMO}}}^N$ is the HOMO energy of the N electron system, and E^{N-1} and E^N are the energy of the $N-1$ and N electron systems, respectively. Accordingly, ω can be adjusted to a given molecular system by minimizing

$$\Delta E(\omega) = {E_{\mathrm{HOMO}}}^N(\omega) + [E^{N-1}(\omega) - E^N(\omega)] \quad (2)$$

In long-range charge transfer systems, the tuning procedure has been modified by including a negatively charged acceptor system. The complete proposed tuning procedure seeks the ω that minimizes the overall deviation expressed in the target function:

$$J^2(\omega) = [{E_{\mathrm{HOMO}}}^N(\omega) + \mathrm{IP}^N(\omega)]^2 + [{E_{\mathrm{HOMO}}}^{N+1}(\omega) + \mathrm{IP}^{N+1}(\omega)]^2 \quad (3)$$

where ${E_{\mathrm{HOMO}}}^{N+1}$ and IP^{N+1} are the HOMO energy and ionization energy, respectively, of the $N+1$ system. It has been shown that the TD-DFT calculations with the tuned LC functionals can be used to obtain highly reliable results even for systems that are problematic for normal TD-DFT calculations.[65−68] It would therefore be of interest to test this newly proposed range-separation tuning procedure for the excited states of the important indole and azaindole molecules.

The aim of the present study is to examine the applicability of TD-DFT methods to describe the lower part of the absorption spectrum of indole and azaindole, which are important prototypes for many biologically important molecules. For this purpose, we carefully selected various different density functionals, including the tuned range-separation LC functionals, and used them with the appropriate basis sets in the present study. Apart from the ^1L_a and ^1L_b $\pi-\pi^*$ states, two other important states, $\pi-\sigma^*$ and $n-\pi^*$, which are supposed to be involved in the photochemistry of these molecules, were also considered in the present study. In addition to indole and azaindole, we have also considered two closely related systems, indene and benzimidazole.

2. COMPUTATIONAL DETAILS

All calculations were performed with the Gaussian 09 suite of programs.[69,70] At first, ground-state structures were optimized followed by frequency calculations by using the B3LYP functional[71,72] with the 6-311+G(d,p) basis set. These frequency calculations showed that the optimized structures are minimum energy on the potential energy surface. Finally, coupled-cluster singles and doubles excitation (CCSD) theory[73−75] was used with the 6-311+G(d,p) basis set to obtain the ground state geometries, which were used for all of the excited state calculations in the present study.

The vertical absorption spectra of indole, azaindole, indene, and benzimidazole were obtained using time-dependent density functional theory[33−36] with different density functionals, which were recommended for excited-state calculations after they were extensively tested for many other systems.[37−39,54,55,57,58,76] The selected functionals include hybrid [B3LYP, PBE0,[77,78] and mPW1PW91 (ref 79)], local meta-GGA [M06-L (ref 80)], global-hybrid meta-GGA [M06-2X (ref 81)], and long-range corrected [CAM-B3LYP,[82] ωB97XD,[83] LC-BLYP,[84] and LC-ωPBE (refs 60, 85−87)] functionals. For convenience, M06-L and M06-2X functionals are denoted as meta-GGA functionals. The system-specific range-separation parameter ω is determined via minimizing the functional given by eq 3 by separately performing necessary ground state calculations, and the tuned range-separation parameter is used for all of the calculations with the LC functionals. For the TD-DFT calculations, the 6-311+G(2d,p) basis set, which has been shown to be adequate enough for the calculation of low-lying excited states of various molecules,[76] was used. Though the main focus of the present study is the valence-excited states, a simultaneous and proper description

of the Rydberg states is required to obtain accurate results. Hence, the TD-DFT calculations were also performed using the 6-311+G(2*d*,*p*) basis set augmented with two sets of Rydberg *sp* functions for carbon and nitrogen.

Because of their biological relevance, it is necessary to accurately estimate their ground state as well as their excited state dipole moments. Moreover, the dipole moments could assist in the differentiation of these two excited states since, as explained earlier, the ^1L_b has a smaller dipole moment similar to the ground state, while ^1L_a has a large dipole moment. For these reasons, we calculated the excited state dipole moments (relaxed) using all of the selected density functionals (except LC-ωPBE functional through which relaxed dipole moments cannot be derived using Gaussian).

3. RESULTS

The schematic structures of the selected systems, indole, azaindole, indene, and benzimidazole, are provided in Figure 1. The system-specific range-separation parameters obtained using the tuning procedure based on eq 3 are almost the same for indole, azaindole, and benzimidazole: the derived optimal ω values are 0.26 a_0^{-1} (for LC-ωPBE), 0.27 a_0^{-1} (for LC-BLYP), and 0.22 a_0^{-1} (for ωB97XD). The calculated ω values, however, vary slightly for indene: 0.25 a_0^{-1} (for LC-ωPBE), 0.26 a_0^{-1} (for LC-BLYP), and 0.21 a_0^{-1} (for ωB97XD). These derived optimal ω values were used for these three LC functionals for all of the calculations in the present study unless otherwise mentioned. In contrast to the fully long-range corrected LC functionals, no minimum is found across a large range of ω values (0.1−1.5 a_0^{-1}) for CAM-B3LYP. As mentioned by Srebro and Autschbach,[88] the inclusion of a pure DFT component in a functional that is not fully long-range corrected to enforce $V_{XC}(\infty) = 0$ may prevent eq 3 from being satisfied. So for the CAM-B3LYP LC functional, we used the default ω (0.33 a_0^{-1}), α (0.19), and β (0.46) values throughout the present study.

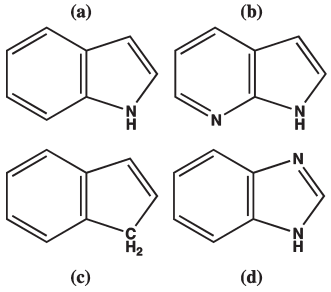

Figure 1. Schematic structures of (a) indole, (b) azaindole, (c) indene, and (d) benzimidazole.

All four selected molecules have C_s symmetry, and hence all the transitions are optically allowed. For each molecule, the vertical ^1L_a and ^1L_b $\pi-\pi^*$ excitation energies were calculated using all nine of the selected density functionals with the 6-311+G(2*d*,*p*) basis set augmented with two sets of Rydberg *sp* functions on carbon and nitrogen atoms (see Tables 1−5). The $\pi-\sigma^*$ state lies close in energy to the ^1L_b and ^1L_a states and plays a crucial role in both the spectroscopic and photophysical effects observed in indole due to its ability to undergo vibronic coupling with the ^1L_a and ^1L_b $\pi-\pi^*$ states and to mediate nonradiative electronic population transfer from the S_1 and S_2 states upon NH bond elongation.[11−13] It is thus also expected to play a crucial role in the photophysics of azaindole as well as those of the derivatives of indole and azaindole molecules, including the all-important tryptophans. It is also possible that the potentially low-lying $n-\pi^*$ states, specifically in azaindole and benzimidazole, might also be involved in the complex photochemistry of these molecules. Hence, the tabulated results also include $\pi-\sigma^*$ (indole), $\pi-\sigma^*$ and $n-\pi^*$ (azaindole and benzimidazole) excitation energies along with the ^1L_a and ^1L_b energies. All of the available theoretical and experimental values were also included in the tables. The calculations were also performed without the Rydberg functions, i.e., with the 6-311+G(2*d*,*p*) basis set, and all of the results are given in the Supporting Information (Table SI.1−4).

Table 1. Calculated Vertical Excitation Energies (ΔE in eV), Oscillator Strengths (f), and Dipole Moments (μ in D) for ^1L_b and ^1L_a States of Indole[a]

	$\pi-\pi^*$ ^1L_b state			$\pi-\pi^*$ ^1L_a state			$\pi-3s$ and $\sigma^*_{(N-H)}$		
method	ΔE	f	μ	ΔE	f	μ	ΔE	f	μ
B3LYP	4.80	0.033	2.41	4.66	0.069	4.05	4.64	0.002	10.60
M06-L	4.77	0.026	2.48	4.57	0.058	4.23	4.64	0.001	12.72
M06-2X	5.01	0.047	2.70	5.05	0.092	3.25	4.94	0.002	10.07
mPW1PW91	4.89	0.038	2.44	4.76	0.073	3.99	4.81	0.002	10.27
PBE0	4.90	0.039	2.49	4.77	0.072	4.05	4.90	0.002	10.48
CAM-B3LYP	4.95	0.037	2.51	4.99	0.101	3.56	5.09	0.003	9.34
ωB97XD	4.99	0.032	2.29	5.05	0.114	3.92	5.43	0.004	8.61
LC-ωPBE	4.89	0.029		4.99	0.097		5.28	0.003	
LC-BLYP	4.87	0.030	2.31	4.96	0.098	3.97	5.04	0.003	8.50
DFT/MRCI[b]	4.62		1.99	4.99		5.82			
CC2[b]	4.87		2.17	5.14		5.69			
CAS-PT2[c]	4.43	0.050	0.85[e]	4.73	0.081	5.69[e]	4.85	0.001	12.31[e]
	(4.30)[d]	(0.02)	(1.55)	(4.65)	(0.09)	(6.12)	(5.05)	(0.00003)	11.03
exptl.[c]	4.37	0.045	1.86[f]	4.77	0.123	5.86			

[a] TD-DFT calculations using the 6-311+G(2*d*,*p*) basis set augmented with two sets of Rydberg diffuse functions [2*s*,2*p*] on C and N at the CCSD/6-311+G(*d*,*p*) optimized structure. [b] Taken from ref 18. [c] CAS-PT2 and experimental values taken from ref 10. [d] Values in parentheses taken from ref 11. [e] Dipole moments calculated from the CASSCF wave functions. [f] Experimental value from ref 89.

dx.doi.org/10.1021/ct200768b | J. Chem. Theory Comput. 2012, 8, 575–584

4. DISCUSSION

4.1. Indole. Table 1 reveals that some of the widely used density functionals interchange the ^1L_a and ^1L_b $\pi-\pi^*$ state ordering in indole. All of the hybrid functionals and the meta-GGA M06-L functional wrongly predict that the ^1L_a state is the lowest excited state in indole and that the ^1L_b state lies in the range of 0.13−0.2 eV above the ^1L_a state. The M06-2X functional predicts the right order of these states but predicts a negligible energy gap between them (0.04 eV). The same value, however, in CAS-PT2 and in the experimental studies is 0.30 and 0.40 eV, respectively.

In contrast to the hybrid and M06-L functionals, all of the LC functionals correctly identify that the ^1L_b state is the lowest state in indole. The transition energies for ^1L_a as obtained using all four LC functionals are overestimated by around 0.3 eV when compared to those of the experimental and CAS-PT2 values. Again, as with the meta-GGA M06-2X functional, the energy gaps between the ^1L_b and ^1L_a states obtained with the LC functionals are very small (0.04−0.1 eV) when compared with the CAS-PT2 and experimental values (0.3−0.4 eV). The ^1L_b excitation energies calculated using all of the functionals are overestimated by around 0.4 to 0.6 eV. Better results are obtained using B3LYP and M06-L functionals. In contrast, the calculated oscillator strengths, irrespective of the density functional used, obey the generally accepted trend: ^1L_a is more intense than the ^1L_b state. Quantitatively, the LC functionals reproduce the experimental values better than the hybrid functionals do.

Like the transition energies, dipole moments of these two $\pi-\pi^*$ states are particularly important because it is known that while the ^1L_b state has a dipole moment value very close to that of the ground state, the dipole moment of the ^1L_a state is more than three times that of the ground state, which would lead to more pronounced solvent effects. The calculated dipole moments of the ^1L_b state agree well with the recently derived experimental value, and in fact these calculated values are better than the CASSCF value.[10] On the other hand, all of the selected density functionals, including the LC functionals, underestimate the dipole moment of ^1L_a state by around 2 D.

To investigate the bulk solvent effects, we calculated the excitation energies of indole with water as a solvent, using the polarizable continuum model (PCM)[91,92] and a nonequilibrium scheme for the TD-DFT calculations.[93] For these calculations, we used 6-311+G(2*d*,*p*) basis set, and the results are tabulated in Table 2. Because the ^1L_a state is more polar than the ^1L_b state, it is preferentially more stabilized by interaction with the water environment. A small displacement of 0.06 eV, on moving from the gas phase to water, is observed experimentally for the ^1L_b state, while the same red shift for the ^1L_a state is 0.18 eV. Although almost all of the functionals nicely reproduce similar red shifts, a closer examination reveals some underlying issues.

Table 2. Calculated Vertical Excitation Energies (ΔE in eV), Oscillator Strengths (f), and Dipole Moments (μ in D) for ^1L_b and ^1L_a States of Indole in Water[a]

	$\pi-\pi^*$ ^1L_b state			$\pi-\pi^*$ ^1L_a state		
method	ΔE	f	μ	ΔE	f	μ
B3LYP	4.77	0.113	3.28	4.52	0.184	6.16
M06-L	4.74	0.084	3.45	4.45	0.148	6.33
M06-2X	4.99	0.160	3.20	4.87	0.246	5.76
mPW1PW91	4.86	0.122	3.28	4.62	0.198	6.08
PBE0	4.86	0.123	3.31	4.63	0.196	6.13
CAM-B3LYP	4.92	0.149	3.21	4.81	0.242	5.55
ωB97XD	4.96	0.159	3.30	4.87	0.246	5.52
LC-ωPBE	4.87	0.057		4.94	0.110	
LC-BLYP	4.85	0.187	3.71	4.78	0.186	5.40
CAS-PT2[b]	4.40		1.55[c]	4.67		7.49[c]
exptl.[b]	4.31			4.59		

[a] TD-DFT calculations using the 6-311+G(2*d*,*p*) basis set at the gas-phase CCSD/6-311+G(*d*,*p*) optimized structure. [b] CAS-PT2 and experimental values taken from ref 10. [c] Dipole moments calculated from the CASSCF wave functions.

Table 3. Calculated Vertical Excitation Energies (ΔE in eV), Oscillator Strengths (f), and Dipole Moments (μ in D) for ^1L_b and ^1L_a States of Azaindole[a]

	$\pi-\pi^*$ ^1L_b state			$\pi-\pi^*$ ^1L_a state			$n-\pi^*$			$\pi-3s$ and $\sigma^*_{(N-H)}$		
method	ΔE	f	μ	ΔE	f	μ	ΔE	f	μ	ΔE	f	μ
B3LYP	4.78	0.083	2.21	4.51	0.062	5.39	5.01	0.003	1.82	5.11	0.004	9.99
M06-L	4.75	0.067	2.31	4.39	0.049	5.36	4.87	0.002	1.91	5.13	0.002	11.50
M06-2X	4.99	0.080	2.22	4.95	0.119	5.04	5.17	0.003	1.84	5.37	0.004	9.13
mPW1PW91	4.86	0.089	2.16	4.63	0.069	5.37	5.10	0.003	1.83	5.27	0.005	9.53
PBE0	4.87	0.090	2.17	4.63	0.068	5.39	5.09	0.003	1.85	5.35	0.005	9.76
CAM-B3LYP	4.92	0.058	2.63	4.88	0.137	4.63	5.32	0.004	1.79	5.51	0.006	9.14
ωB97XD	4.96	0.036	4.12	4.93	0.165	3.08	5.34	0.004	1.81	5.80	0.008	8.35
LC-ωPBE	4.83	0.040		4.86	0.137		5.09	0.003		5.67	0.006	
LC-BLYP	4.82	0.050	2.95	4.85	0.131	4.46	5.11	0.004	1.75	5.44	0.006	8.09
DFT/MRCI[b]	4.52			4.74								
RICC2[b]	4.82			5.00								
CAS-PT2[b]	4.22	0.043	1.61[e]	4.49	0.072	6.39[e]	5.27	0.008	2.04[e]			
	(4.44)[d]	(0.049)		(4.92)	(0.069)							
exptl.[c]	4.29		2.30[f]	4.49			4.56[g]	<0.01[g]				

[a] TD-DFT using the 6-311+G(2*d*,*p*) basis set augmented with two sets of Rydberg diffuse functions [2*s*,2*p*] on C and N at the CCSD/6-311+G(*d*,*p*) optimized structure. [b] Taken from ref 32. [c] CAS-PT2 and experimental values taken from ref 15. [d] Values in parentheses taken from ref 20. [e] Dipole moments calculated from the CASSCF wave functions. [f] Experimental value taken from ref 17. [g] Experimental $n-\pi^*$ values taken from ref 16.

All of the hybrid and meta-GGA functionals (including M06-2X, in contrast to the gas phase in this case) predict a wrong order of states in the condensed phase calculations. The two $\pi-\pi^*$ states are interchanged in the CAM-B3LYP, ωB97XD, and LC-BLYP LC functionals. Moreover, although the LC-ωPBE functional could reproduce a correct order of states, the calculated energy difference between the ^1L_b and ^1L_a states is not close to the experimental value.

4.2. Azaindole. The excitation energies computed for the important states in azaindole are given in Table 3. As in the case of indole, the two $\pi-\pi^*$ states are interchanged in most of the TD-DFT calculations, including some that did predict the correct order for indole (i.e., the meta-GGA M06-2X and LC CAM-B3LYP and ωB97XD). It should be noticed that the energy gap between the two $\pi-\pi^*$ states in indole is larger by around 0.1−0.2 eV than in azaindole, which might have helped these functionals to predict the correct order in the former case. Only two of the LC functionals, LC-ωPBE and LC-BLYP, correctly predicted that ^1L_b is the lowest excited state in azaindole, and even in these cases the calculated energy gap (0.03 eV) between the two $\pi-\pi^*$ states differs substantially from the experimental (0.20 eV) and CAS-PT2 (0.27 eV) values. The oscillator strengths calculated using B3LYP, M06-L, mPW1PW91, and PBE0 functionals indicate that the ^1L_b $\pi-\pi^*$ transition is more intense than the other $\pi-\pi^*$ excitation, which is contrary to the generally accepted trend. Though the dipole moments calculated for the ^1L_b state using all of the functionals (except ωB97XD, which wrongly predicts that the ^1L_b state has a larger dipole moment) agree with the CAS-PT2 value, those calculated for the ^1L_a state using LC functionals are less accurate.

It is widely believed in the case of indole that ^1L_b is basically an intrabenzenic ring transition but ^1L_a is essentially an internal charge-transfer-like transition from the five-membered pyrrolic ring to the six-membered benzenic ring. In the study on nonlinear PAHs, Richard and Herbert[57] suggested that ^1L_a excitations have a partial charge-transfer character. However, standard diagnosis tools did not indicate that ^1L_a has any more CT character than does ^1L_b.[57] So the nature of the ^1L_a states in PAHs is still not well understood. To understand the nature of these two $\pi-\pi^*$ states in indole and azaindole, we calculated the Mulliken charge differences between the ground state (S_0) and the excited states (^1L_a and ^1L_b), using the B3LYP functional, and the results are given in Figure 2. Comparing the charge differences between $S_0 \rightarrow {}^1L_b$ and $S_0 \rightarrow {}^1L_a$ excitations indicates a significant disparity between them. In the case of the $S_0 \rightarrow {}^1L_a$ transition, some extra negative charge is accumulated in the benzene (pyridine) ring in indole (azaindole), which is absent in the $S_0 \rightarrow {}^1L_b$ excitation. In other words, ^1L_a appears to be a kind of internal charge-transfer state. [For the indole case, our calculations also showed a similar kind of disparity (see Figure SI.1) in charge differences between these two transitions when the solvent effect is included].

To further check the difference in nature of these two states, we examined the electron density differences [$\Delta\rho$ = ρ(excited state) − ρ(ground state)], and the resulting isosurface (obtained mainly with 0.02 isovalues) representations, computed using TD-B3LYP, are provided in Figure 3. A careful observation

Table 4. Calculated Vertical Excitation Energies (ΔE in eV), Oscillator Strengths (f), and Dipole Moments (μ in D) for ^1L_b and ^1L_a States of Indene[a]

	$\pi-\pi^*$ ^1L_b state			$\pi-\pi^*$ ^1L_a state		
method	ΔE	f	μ	ΔE	f	μ
B3LYP	4.68	0.013	1.13	4.86	0.179	0.83
M06-L	4.61	0.008	0.95	4.81	0.160	1.17
M06-2X	4.99	0.010	1.09	5.16	0.207	0.58
mPW1PW91	4.78	0.014	1.12	4.96	0.184	0.72
PBE0	4.79	0.013	1.13	4.97	0.187	0.72
CAM-B3LYP	4.93	0.011	1.08	5.07	0.192	0.57
ωB97XD	4.97	0.007	1.06	5.10	0.198	0.59
LC-ωPBE	4.87	0.000		5.09	0.209	
LC-BLYP	4.85	0.001	1.06	5.07	0.212	0.46
CAS-PT2[b]	4.46	0.000	0.20[c]	5.02	0.175	1.46[c]
exptl.[b]	4.4	0.003		5.0	0.194	

[a] TD-DFT calculations using the 6-311+G(2d,p) basis set augmented with two sets of Rydberg diffuse functions [2s,2p] on C and N at the CCSD/6-311+G(d,p) optimized structure. [b] CAS-PT2 and experimental values taken from ref 90. [c] Dipole moments calculated from the CASSCF wave functions.

Table 5. Calculated Vertical Excitation Energies (ΔE in eV), Oscillator Strengths (f), and Dipole Moments (μ in D) for ^1L_b and ^1L_a States of Benzimidazole[a]

	$\pi-\pi^*$ ^1L_b state			$\pi-\pi^*$ ^1L_a state			$n-\pi^*$			$\pi-3s$ and $\sigma^*_{(N-H)}$		
method	ΔE	f	μ	ΔE	f	μ	ΔE	f	μ	ΔE	f	μ
B3LYP	4.92	0.055	3.22	5.13	0.086	3.62	5.73	0.000	6.17	5.18	0.001	10.70
M06-L	4.89	0.043	3.11	5.06	0.080	3.68	5.44	0.000	4.86	5.14	0.001	13.50
M06-2X	5.14	0.068	3.31	5.48	0.098	3.51	6.18	0.001	2.29	5.52	0.001	9.49
mPW1PW91	5.01	0.059	3.27	5.24	0.088	3.62	5.89	0.002	5.09	5.36	0.001	10.42
PBE0	5.01	0.059	3.28	5.25	0.088	3.66	5.88	0.001	3.87	5.45	0.001	10.48
CAM-B3LYP	5.07	0.065	3.42	5.38	0.090	3.65	6.17	0.001	2.90	5.68	0.000	8.63
ωB97XD	5.10	0.066	3.47	5.44	0.091	3.73	6.21	0.001	2.87	6.04	0.000	7.54
LC-ωPBE	5.00	0.059		5.39	0.088		5.85	0.001		5.87	0.000	
LC-BLYP	4.98	0.058	3.43	5.36	0.090	3.78	5.86	0.001	3.22	5.62	0.000	7.65
CAS-PT2[b]	4.56	0.040	2.94[c]	4.99	0.118	5.26[c]	6.09	0.000	1.19[c]			
exptl.[b]	4.5			5.0								

[a] TD-DFT calculations using the 6-311+G(2d,p) basis set augmented with two sets of Rydberg diffuse functions [2s,2p] on C and N at the CCSD/6-311+G(d,p) optimized structure. [b] CAS-PT2 and experimental values taken from ref 15. [c] Dipole moments calculated from the CASSCF wave functions.

dx.doi.org/10.1021/ct200768b | J. Chem. Theory Comput. 2012, 8, 575–584

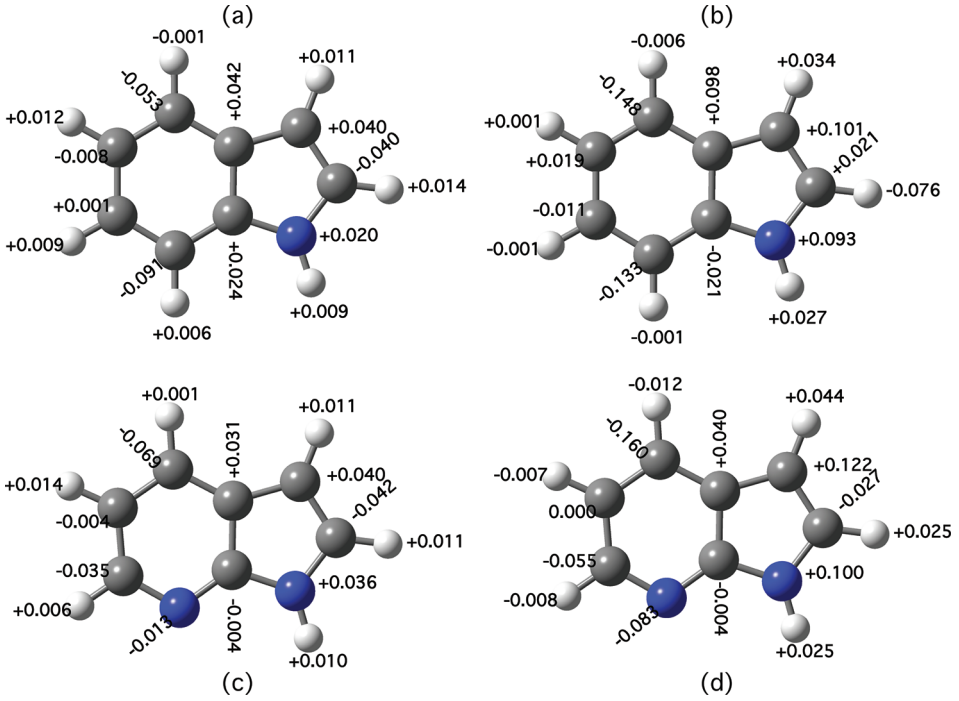

Figure 2. Difference in atomic charges due to (a) $S_0 \rightarrow L_b$ (π^*) excitation in indole, (b) $S_0 \rightarrow L_a$ (π^*) excitation in indole, (c) $S_0 \rightarrow L_b$ (π^*) excitation in azaindole, and (d) $S_0 \rightarrow L_a$ (π^*) excitation in azaindole.

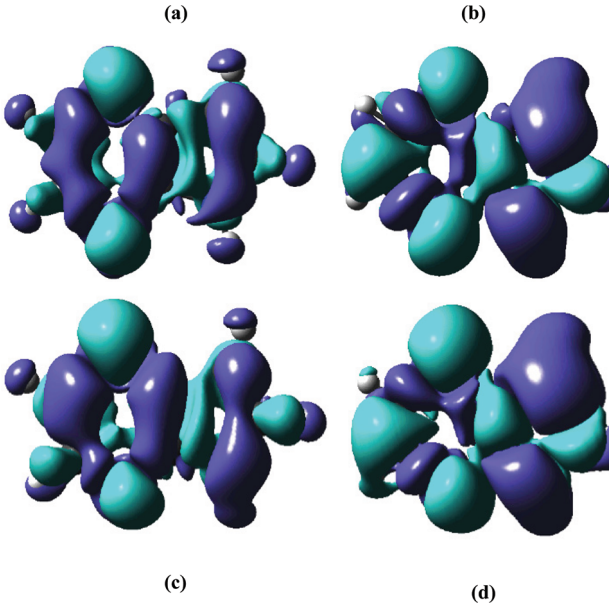

Figure 3. Difference in electron density due to (a) $S_0 \rightarrow L_b$ (π^*) excitation in indole, (b) $S_0 \rightarrow L_a$ (π^*) excitation in indole, (c) $S_0 \rightarrow L_b$ (π^*) excitation in azaindole, and (d) $S_0 \rightarrow L_a$ (π^*) excitation in azaindole. Green represents electron gain.

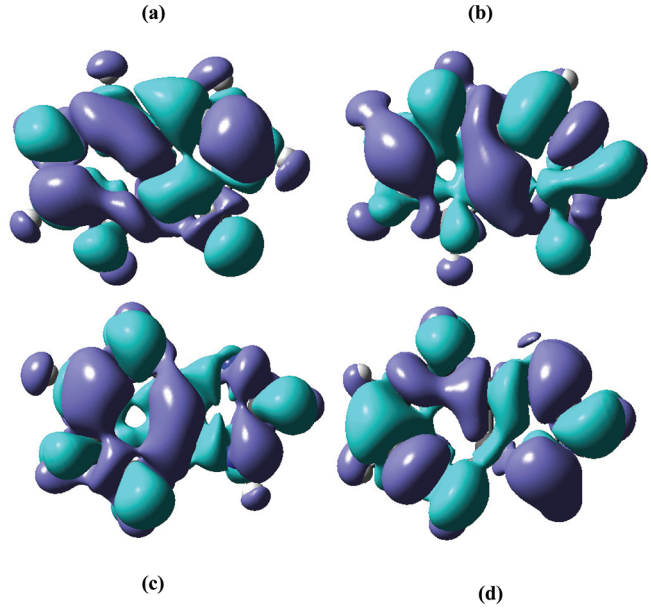

Figure 4. Difference in electron density due to (a) $S_0 \rightarrow L_b$ (π^*) excitation in indene, (b) $S_0 \rightarrow L_a$ (π^*) excitation in indene, (c) $S_0 \rightarrow L_b$ (π^*) excitation in benzimidazole, and (d) $S_0 \rightarrow L_a$ (π^*) excitation in benzimidazole. Green represents electron gain.

reveals that a substantial charge transfer from the pyrrole to benzene (pyridine) ring in indole (azaindole) results from the $S_0 \rightarrow {}^1L_a$ transition; however, such a relocation of charges is not seen in the ${}^1L_b$ state. These differences in charge transfer, when combined with the fact that conventional TD-DFT methods overstabilize the charge-transfer states, could explain why the hybrid functionals underestimate the ${}^1L_a$ state in indole and azaindole, causing it to become the first excited state.

4.3. Indene and Benzimidazole. Contrary to the case of indole and azaindole molecules, all of the density functionals predict correct order of ${}^1L_b$ and ${}^1L_a$ states in indene (see Table 4) and benzimidazole (see Table 5). However, once again the energy differences between these two states are computed to

dx.doi.org/10.1021/ct200768b | J. Chem. Theory Comput. 2012, 8, 575–584

Table 6. Calculated Vertical Excitation Energies (ΔE in eV), Oscillator Strengths (f), and Dipole Moments (μ in D) for ^1L_b and ^1L_a States of Indole and Azaindole[a]

	$\pi-\pi^*$ ^1L_b state			$\pi-\pi^*$ ^1L_a state			$n-\pi^*$			$\pi-3s$ and $\sigma^*_{(N-H)}$		
method	ΔE	f	μ	ΔE	f	μ	ΔE	f	μ	ΔE	f	μ
					indole							
LC-ωPBE	5.07	0.037		5.24	0.121					5.80	0.004	
	4.89	*0.029*		*4.99*	*0.097*					*5.28*	*0.003*	
LC-BLYP	5.10	0.042	2.22	5.24	0.124	3.56				5.66	0.004	7.69
	4.87	*0.030*	*2.31*	*4.96*	*0.098*	*3.97*				*5.04*	*0.003*	*8.50*
ωB97XD	4.97	0.034	2.45	5.02	0.106	3.80				5.35	0.004	8.99
	4.99	*0.032*	*2.29*	*5.05*	*0.114*	*3.92*				*5.43*	*0.004*	*8.61*
					azaindole							
LC-ωPBE	4.98	0.133		5.19	0.087		5.48	0.004		6.17	0.008	
	4.83	*0.040*		*4.86*	*0.137*		*5.09*	*0.003*		*5.67*	*0.006*	
LC-BLYP	5.01	0.149	2.06	5.24	0.084	4.57	5.61	0.004	1.75	6.04	0.009	7.30
	4.82	*0.050*	*2.95*	*4.85*	*0.131*	*4.46*	*5.11*	*0.004*	*1.75*	*5.44*	*0.006*	*8.09*
ωB97XD	4.93	0.061	2.58	4.89	0.134	4.72	5.30	0.004	1.82	5.72	0.008	8.71
	4.96	*0.036*	*4.12*	*4.93*	*0.165*	*3.08*	*5.34*	*0.004*	*1.81*	*5.80*	*0.008*	*8.35*

[a] TD-DFT calculations using LC functionals with the default range-separation parameter and using the 6-311+G(2d,p) basis set augmented with two sets of Rydberg diffuse functions [2s,2p] on C and N at the CCSD/6-311+G(d,p) optimized structure. Values in italics were obtained using tuned range-separation parameters.

be much smaller than the available experimental and CAS-PT2 values. While the oscillator strengths for both of the states were accurately calculated (^1L_a state is more intense) by all the functionals, the dipole moments were not. In the case of indene, most of the density functionals indicate that the ^1L_b state has a larger dipole moment than its counterpart ^1L_b state that is contradictory with the CAS-PT2 result. In the case of benzimidazole, both of the states are computed to have similar dipole moments, whereas the ^1L_a state is predicted to have double the dipole moment of ^1L_b by the CAS-PT2 calculation.

Isosurface (obtained mainly with 0.02 isovalues) representations of the difference in electron densities due to $S_0 \rightarrow {}^1L_b$ and $S_0 \rightarrow {}^1L_a$ transitions in indene and benzimidazole are shown in Figure 4. The charge-transfer from the pyrrole ring to benzene (pyridine) ring in indole (azaindole) seen in the $S_0 \rightarrow {}^1L_a$ transition is absent in indene. In other words, both the states have similar local intraring charge reorganization. Even in benzimidazole, the apparent difference seen in the nature of $S_0 \rightarrow {}^1L_b$ and $S_0 \rightarrow {}^1L_a$ transitions in indole and azaindole is not clearly seen, or at least inter-ring charge transfer in $S_0 \rightarrow {}^1L_a$ transition is less pronounced. Hence, it appears that the reduced charge-transfer character of ^1L_a states in indene and benzimidazole enable the hybrid density functionals to correctly reproduce the order of ^1L_a and ^1L_b states. It should be also noted that the energy gap between these two states in indene and benzimidazole is larger than that in indole and azaindole.

4.4. Excitation Energies. The calculated vertical excitation energy would be comparable directly to the experimental value if the transition were the origin transition. However, this is not the case for the considered systems, except in indole, where the value observed for the ^1L_b state in the experimental studies (4.37 eV) corresponds to the ^1L_b band origin and maximum, and the experimental value for the ^1L_a state (4.77 eV) represents the ^1L_a band origin. Also, we have reliable *ab initio* excitation energies only for the indole and azaindole molecules; hence comparisons should be made carefully. It could be concluded that excitation energies obtained for the ^1L_b state are overestimated in all the functionals. The ^1L_a states, on the other hand, are underestimated by the hybrid functionals and the meta-GGA M06-L functional, and because of that, all of them incorrectly predict the order of states in indole and azaindole. Despite correctly identifying the state order, the LC functionals overestimate the ^1L_a states. And in fact, CAM-B3LYP and wB97XD functionals are unable to predict the right order of states in azaindole. The M06-2X functional seems exceptional: contrary to the other selected hybrid and meta-GGA functionals, it does not underestimate the ^1L_a state; however, the excitation energy obtained for the ^1L_b state is around 0.2 eV higher than those predicted by the other hybrid functionals. The energy gap between these two $\pi-\pi^*$ states, which has a greater significance for their spectroscopy, is not reliably computed by almost all of the selected density functionals.

4.5. The $\pi-\sigma^*$ and $n-\pi^*$ States. The excitation energies calculated for the $\pi-\sigma^*$ state in indole, azaindole, and benzimidazole, are also given in Tables 1, 3, and 5. Earlier investigations concluded that this state plays an important role in the photochemistry of indole and hence may be expected to play a similar role in azaindole and in benzimidazole also. Earlier studies also showed that the wave function of the lowest Rydberg state is dominated by electronic configuration $\pi \rightarrow \sigma^*$, which is the lowest $\pi-\sigma^*$ Rydberg-like state with the σ^* orbital essentially localized on the NH moiety and having a node along the NH bond. We also found the same nature of this $\pi-\sigma^*$ state in all three of these molecules, and so we denote this state as $\pi-3s$ and $\sigma^*(N-H)$. Comparing the calculated $\pi-\sigma^*$ excited state energy with the available values (available only for the indole case), we find that all of the global hybrid functionals underestimate the excitation energy for this state. By considering the nature of the state ($\pi-3\sigma$ Rydberg-like nature) and its large calculated dipole moments, it should be a charge-transfer-like state, which is why all of the hybrid density functionals underestimate it. The LC functionals, especially LC-ωPBE and ωB97XD, overestimate the

dx.doi.org/10.1021/ct200768b | J. Chem. Theory Comput. 2012, 8, 575–584

Table 7. Calculated Vertical Excitation Energies (ΔE in eV), Oscillator Strengths (f), and Dipole Moments (μ in D) for ^1L_b and ^1L_a States of Indene and Benzimidazole[a]

	$\pi-\pi^*$ ^1L_b state			$\pi-\pi^*$ ^1L_a state			$n-\pi^*$			$\pi-3s$ and $\sigma^*_{(N-H)}$		
method	ΔE	f	μ	ΔE	f	μ	ΔE	f	μ	ΔE	f	μ
					indene							
LC-ωPBE	5.11	0.000		5.26	0.199							
	4.87	*0.000*		*5.09*	*0.209*							
LC-BLYP	5.14	0.001	1.03	5.25	0.192	0.47						
	4.85	*0.001*	*1.06*	*5.07*	*0.212*	*0.46*						
ωB97XD	4.96	0.007	1.07	5.09	0.198	0.53						
	4.97	*0.007*	*1.06*	*5.10*	*0.198*	*0.59*						
					benzimidazole							
LC-ωPBE	5.17	0.064		5.60	0.089		6.38	0.000		6.41	0.000	
	5.00	*0.059*		*5.39*	*0.088*		*5.85*	*0.001*		*5.87*	*0.000*	
LC-BLYP	5.20	0.068	3.56	5.59	0.087	3.74	6.54	0.003	2.14	6.26	0.000	7.13
	4.98	*0.058*	*3.43*	*5.36*	*0.090*	*3.78*	*5.86*	*0.001*	*3.22*	*5.62*	*0.000*	*7.65*
ωB97XD	5.09	0.065	3.45	5.41	0.091	3.72	6.16	0.001	3.01	5.96	0.001	7.88
	5.10	*0.066*	*3.47*	*5.44*	*0.091*	*3.73*	*6.21*	*0.001*	*2.87*	*6.04*	*0.000*	*7.54*

[a] TD-DFT calculations using LC functionals with the default range-separation parameter and using the 6-311+G(2d,p) basis set augmented with two sets of Rydberg diffuse functions [2s,2p] on C and N at the CCSD/6-311+G(d,p) optimized structure. Values in italics were obtained using tuned range-separation parameters.

excitation energy of the state. Also, the dipole moments calculated using LC functionals were underestimated.

The excitation energies calculated for the $n-\pi^*$ state in azaindole and benzimidazole are also given in Tables 3 and 5. Ilich[16] reported the absorption spectrum of azaindole in an argon matrix and predicted the second transition ($1^1A''$) to be of $n\rightarrow\pi^*$ character with 4.55 eV transition energy with a very weak intensity (<0.01), and perpendicular to the molecular plane. However, CAS-PT2 calculations by Serrano-Andres and Borin[8,15] did not support this fact because this state has been calculated at 5.27 eV. Our calculated excitation energies for this $n-\pi^*$ state in azaindole are mostly close to the value calculated by the CAS-PT2. Overall, the $n-\pi^*$ state energies in azaindole and benzimidazole obtained by the LC functionals, especially CAM-B3LYP and ωB97XD functionals, are relatively larger than those obtained using the hybrid and meta-GGA functionals.

4.6. Influence of Tuning the LC Range Parameter. To examine how far the tuned system-specific range-separation parameter influenced the calculated excitation energies, we have compared the excitation energies of the four selected molecules as obtained by using LC-ωPBE, LC-BLYP, and ωB97XD functionals with their tuned ω values (as reported above) and with their default ω values. The Gaussian default ω values for LC-ωPBE, LC-BLYP, and ωB97XD functionals are 0.4, 0.47, and 0.2 a_0^{-1}, respectively. The same basis set, 6-311+G(2d,p) augmented with two sets of Rydberg diffuse functions [2s,2p] on C and N, is used for this purpose. The calculated excitation energies along with the respective values obtained using the tuned ω are tabulated in Tables 6 and 7.

The results obtained using the ωB97XD LC functional with the default ω value are almost the same as those with the system-specific tuned ω value, thanks to the closeness between the tuned (0.21−0.22) and default (0.2) ω values. However, for the other two LC functionals, the tuned ω values are significantly different from their default values. The calculated ^1L_b excitation energies for indole and azaindole, using these two LC functionals with the default ω values, are 0.15 to 0.23 eV higher than those obtained using the tuned ω values. The same difference is 0.25 to 0.39 eV for ^1L_a states, which means that all of these excitation energies are highly overestimated with regard to the default values, and tuning the ω values does indeed improve these two $\pi-\pi^*$ excitation energies significantly. Additionally, the oscillator strengths calculated using these two functionals (with default ω values) predict that the ^1L_b $\pi-\pi^*$ transition (in azaindole) is more intense than the other $\pi-\pi^*$ excitation, which is contrary to the generally accepted trend. Again, the excitation energies calculated for the other two states, $\pi-\sigma^*$ and $n-\pi^*$, using the default ω values are also 0.39 to 0.63 eV higher than the respective values obtained with the tuned ω values. Similar trends are also noticed with the indene and benzimidazole systems (see Table 7). All of these results clearly indicate that better results could be derived using LC functionals with the optimal system-specific range-separation parameter values obtained using the first-principle tuning procedure than with the default ω values.

5. CONCLUDING REMARKS

Nine different popular density functionals, including three hybrid, two meta-GGA, and four long-range corrected functionals with the tuned range-separation parameters, are used to study the all-important ^1L_a and ^1L_b $\pi-\pi^*$ states in the biologically important molecules indole, azaindole, indene, and benzimidazole. None of the selected functionals reliably reproduce all four properties: the order of the ^1L_a and ^1L_b states, the energy gap between these two $\pi-\pi^*$ states, the oscillator strengths, and the dipole moments. The excitation energies computed for the ^1L_b state using some of the hybrid functionals are more accurate than those obtained using LC functionals; however, all of the hybrid functionals failed to reproduce ^1L_b state as the lowest excited state in indole and azaindole correctly. Though LC functionals generally produce the right order of states, this is not true for all of the functionals, and in any case the calculated energy gap

between the two $\pi-\pi^*$ states is severely underestimated. Contrary to the indole and azaindole cases, all of the functionals, including global hybrid functionals, correctly identify the ^1L_b state as the first exited state in both indene and benzimidazole. The difference in electron densities and Mulliken charges due to the ground state → excited state transitions indicate that the ^1L_a state has the involvement of some sort of charge transfer from pyrrole to benzene (pyridine) in indole (azaindole); however, such an inter-ring charge transfer in the ^1L_a transition in indene and benzimidazole is negligible or absent. This charge transfer nature could be blamed for the error of hybrid and meta-GGA functionals, but this might not be the only reason for the errors found in the present study. In any case, it is does appear to be possible to say "yes" in answer to the title question for the functionals studied. Finally, it is worth noting that recent results in the literature[51,76,94−96] have shown that double-hybrid density functionals may offer improved performance over global hybrid and LC functionals for related problems, though not without some reservations,[97] and it would be of interest to test this class of functionals on the systems of the present work.

■ ASSOCIATED CONTENT

Supporting Information. Vertical excitation energies, oscillator strengths, and dipole moments of all the systems using the 6-311+G(2*d*,*p*) basis set and a figure representing differences in atomic charges due to the transitions in indole in water solution. This material is available free of charge via the Internet at http://pubs.acs.org.

■ AUTHOR INFORMATION

Corresponding Author

*E-mail: raja@rsc.anu.edu.au; mcoote@rsc.anu.edu.au.

Notes

The authors declare no competing financial interest.

■ ACKNOWLEDGMENT

We gratefully acknowledge the Australian Research Council for the funding under their centers of Excellence program and generous allocations of Supercomputing time on the National Facility of the Australian National Computational Infrastructure. MLC acknowledges an ARC Future Fellowship.

■ REFERENCES

(1) The, C. K.; Sipior, J.; Sulkes, M. *J. Phys. Chem.* **1989**, *93*, 5393–5400.
(2) Eftink, M. R. *Methods Biochem. Anal.* **1991**, *35*, 127–205.
(3) Lakowicz, J. *Principles of Fluorescence Spectroscopy*, 2nd ed.; Plenum: New York, 1999.
(4) Callis, P. R. *Methods Enzymol.* **1997**, *278*, 113–150.
(5) Vivian, J. T.; Callis, P. R. *Biophys. J.* **2001**, *80*, 2093–2109.
(6) Negrerie, M.; Bellefeuille, S. M.; Whitham, S.; Petrich, J. W.; Thornburg, R. W. *J. Am. Chem. Soc.* **1990**, *112*, 7419–7421.
(7) Callis, P. R.; Vivian, J. T.; Slater, L. S. *Chem. Phys. Lett.* **1995**, *244*, 53–58.
(8) Serrano-Andres, L.; Borin, A. C. *Chem. Phys.* **2000**, *262*, 267–283.
(9) Schmitt, M.; Ratzer, C.; Kleinermanns, K.; Meerts, W. L. *Mol. Phys.* **2004**, *102*, 1605–1614.
(10) Serrano-Andres, L.; Roos, B. O. *J. Am. Chem. Soc.* **1996**, *118*, 185–195.
(11) Sobolewski, A. L.; Domcke, W. *Chem. Phys. Lett.* **1999**, *315*, 293–298.
(12) Sobolewski, A. L.; Domcke, W.; Dedonder-Lardeux, C.; Jouver, C. *Phys. Chem. Chem. Phys.* **2002**, *4*, 1093–1100.
(13) Dian, B. C.; Longarte, A.; Zwier, T. S. *J. Chem. Phys.* **2003**, *118*, 2696–2706.
(14) Nix, M. G. D.; Devine, A. L.; Cronin, B.; Ashfold, M. N. R. *Phys. Chem. Chem. Phys.* **2006**, *8*, 2610–2618.
(15) Borin, A. C.; Serrano-Andres, L. *Chem. Phys.* **2000**, *262*, 253–265.
(16) Ilich, P. *J. Mol. Struct.* **1995**, *354*, 37–47.
(17) Kang, C. K.; Yi, J. T.; Pratt, D. W. *Chem. Phys. Lett.* **2006**, *423*, 7–12.
(18) Brand, C.; Kupper, J.; Pratt, D. W.; Meerts, W. L.; Krugler, D.; Tatchen, J.; Schmitt, M. *Phys. Chem. Chem. Phys.* **2010**, *12*, 4968–4979.
(19) Kupper, J.; Pratt, D. W.; Meerts, W. L.; Brand, C.; Tatchen, J.; Schmitt, M. *Phys. Chem. Chem. Phys.* **2010**, *12*, 4980–4988.
(20) Brause, R.; Schmitt, M.; Krugler, D.; Kleinermanns, K. *Mol. Phys.* **2004**, *102*, 1615–1623.
(21) Taylor, C. A.; El-Bayoumi, M. A.; Kasha, M. *Proc. Nat. Acad. Sci. U. S. A.* **1969**, *63*, 253–260.
(22) Douhal, A.; Kim, S. K.; Zewail, A. H. *Nature* **1995**, *378*, 260–263.
(23) Takeuchi, S.; Tahara, T. *Proc. Natl. Acad. Aci. U. S. A.* **2007**, *104*, 5285–5290.
(24) Kwon, O.-H.; Zewail, A. H. *Proc. Natl. Acad. Sci. U. S. A.* **2007**, *104*, 8703–8708.
(25) Sekiya, H.; Sakota, K. *J. Photochem. Photobiol. C* **2008**, *9*, 81–91.
(26) Yu, X.-F.; Yamazaki, S.; Taketsugu, T. *J. Chem. Theory Comput.* **2011**, *7*, 1006–1015.
(27) Platt, J. R. *J. Chem. Phys.* **1949**, *17*, 484–496.
(28) Lami, H.; Glasser, N. *J. Chem. Phys.* **1986**, *84*, 597–604.
(29) Arnold, S.; Sulkes, M. *J. Phys. Chem.* **1992**, *96*, 4768–4778.
(30) Tubergen, M. J.; Levy, D. H. *J. Phys. Chem.* **1991**, *95*, 2175–2181.
(31) Short, K. W.; Callis, P. R. *J. Chem. Phys.* **2000**, *113*, 5235–5244.
(32) Svartsov, Y. N.; Schmitt, M. *J. Chem. Phys.* **2008**, *128*, No 214310.
(33) Stratmann, R. E.; Scuseria, G. E.; Frisch, M. J. *J. Chem. Phys.* **1998**, *109*, 8218–8224.
(34) Bauernschmitt, R.; Ahlrichs, R. *Chem. Phys. Lett.* **1996**, *256*, 454–464.
(35) Casida, M. E.; Jamorski, C.; Casida, K. C.; Salahub, D. R. *J. Chem. Phys.* **1998**, *108*, 4439–4449.
(36) Dreuw, A.; Head-Gordon, M. *Chem. Rev.* **2005**, *105*, 4009–4037.
(37) Dierksen, M.; Grimme, S. *J. Chem. Phys.* **2004**, *120*, 3544–3554.
(38) Silva-Junior, M. R.; Schreiber, M.; Sauer, S. P.; Thiel, W. *J. Chem. Phys.* **2008**, *129*, No. 104103.
(39) Jacquemin, D.; Perpete, E. A.; Ciofini, I.; Adamo, C.; Valero, R.; Zhao, Y.; Truhlar, D. G. *J. Chem. Theory Comput.* **2010**, *6*, 2071–2085.
(40) Dreuw, A.; Weisman, J. L.; Head-Gordon, M. *J. Chem. Phys.* **2003**, *119*, 2943–2946.
(41) Dreuw, A.; Head-Gordon, M. *J. Am. Chem. Soc.* **2004**, *126*, 4007–4016.
(42) Lange, A. W.; Herbert, J. M. *J. Am. Chem. Soc.* **2009**, *131*, 3913–3922.
(43) Neugebauer, J.; Louwerse, M. J.; Baerends, E. J.; Wesolowski, T. A. *J. Chem. Phys.* **2005**, *122*, No 094115.
(44) Lange, A.; Herbert, J. M. *J. Chem. Theory Comput.* **2007**, *3*, 1680–1690.
(45) Rohrdanz, M. A.; Martins, K. M.; Herbert, J. M. *J. Chem. Phys.* **2009**, *130*, No 054112.
(46) Tozer, D. J.; Amos, R. D.; Handy, N. C.; Roos, B. O.; Serrano-Andres, L. *Mol. Phys.* **1999**, *97*, 859–868.
(47) Grimme, S.; Parac, M. *Chem. Phys. Chem* **2003**, *4*, 292–295.
(48) Parac, M.; Grimme, S. *Chem. Phys.* **2003**, *292*, 11–21.
(49) Catalan, J.; del Valle, J. C.; Kasha, M. *Proc. Natl. Acad. Sci. U.S.A.* **1999**, *96*, 8338–8343.

(50) Catalan, J.; Perez, P.; del Valle, J. C.; de Paz, J. L. G.; Kasha, M. *Proc. Natl. Acad. Sci. U.S.A.* **2002**, *99*, 5799–5803.
(51) Catalan, J.; Perez, P.; del Valle, J. C.; de Paz, J. L. G.; Kasha, M. *Proc. Natl. Acad. Sci. U.S.A.* **2004**, *101*, 419–422.
(52) Catalan, J.; de Paz, J. L. G. *J. Chem. Phys.* **2005**, *123*, No 114302.
(53) Sakota, K.; Jouvet, C.; Dedonder, C.; Fujii, M.; Sekiya, H. *J. Phys. Chem. A* **2010**, *114*, 11161–11166.
(54) Jacquemin, D.; Perpete, E. A.; Scuseria, G. E.; Ciofini, I.; Adamo, C. *J. Chem. Theory Comput.* **2008**, *4*, 123–135.
(55) Jacquemin, D.; Perpete, E. A.; Ciofini, I.; Adamo, C. *Theor. Chem. Acc.* **2011**, *128*, 127–136. See also the references therein.
(56) Goerigk, L.; Grimme, S. *J. Chem. Phys.* **2010**, *132*, No 184103.
(57) Richard, R. M.; Herbert, J. M. *J. Chem. Theory Comput.* **2011**, *7*, 1296–1306. Also see the references therein.
(58) Wong, B. M.; Hsieh, T. H. *J. Chem. Theory Comput.* **2010**, *6*, 3704–3712.
(59) Yu, X.-F.; Yamazaki, S.; Taketsugu, T. *J. Chem. Theory Comput.* **2011**, *7*, 1006–1015.
(60) Vydrov, O. A.; Heyd, J.; Krukau, A.; Scuseria, G. E. *J. Chem. Phys.* **2006**, *125*, No 074106.
(61) Peach, M. J. G.; Helgaker, T.; Salek, P.; Keal, T. W.; Lutnaes, O. B.; Tozer, G. J.; Handy, N. C. *Phys. Chem. Chem. Phys.* **2006**, *8*, 558–562.
(62) Peach, M. J. G.; Cohen, A. J.; Tozer, D. J. *Phys. Chem. Chem. Phys.* **2006**, *8*, 4543–4549.
(63) Rohrdanz, M. A.; Herbert, J. M. *J. Chem. Phys.* **2008**, *129*, No. 034107.
(64) Scherbin, D.; Ruud, K. *Chem. Phys.* **2008**, *349*, 234–243.
(65) Stein, T.; Kronik, L.; Baer, R. *J. Am. Chem. Soc.* **2009**, *131*, 2818–2820.
(66) Stein, T.; Kronik, L.; Baer, R. *J. Chem. Phys.* **2009**, *131*, No. 244119.
(67) Stein, T.; Eiserberg, H.; Kronik, L.; Baer, R. *Phys. Rev. Lett.* **2010**, *105*, No. 266802.
(68) Kuritz, N.; Stein, T.; Baer, R.; Kronik, L. *J. Chem. Theory Comput.* **2011**, *7*, 2408–2415.
(69) Frisch, M. J.; Trucks, G. W.; Schlegel, H. B.; Scuseria, G. E.; Robb, M. A.; Cheeseman, J. R.; Scalmani, G.; Barone, V.; Mennucci, B.; Petersson, G. A.; Nakatsuji, H.; Caricato, M.; Li, X.; Hratchian, H. P.; Izmaylov, A. F.; Bloino, J.; Zheng, G.; Sonnenberg, J. L.; Hada, M.; Ehara, E.; Toyota, K.; Fukuda, R.; Hasegawa, J.; Ishida, M.; Nakajima, T.; Honda, Y.; Kitao, O.; Nakai, H.; Vreven, T.; Montgomery, J. A., Jr.; Peralta, J. E.; Ogliaro, F.; Bearpark, M.; Heyd, J. J.; Brothers, E.; Kudin, K. N.; Staroverov, V. N.; Kobayashi, R.; Normand, J.; Raghavachari, K.; Rendell, A.; Burant, J. C.; Iyengar, S. S.; Tomasi, J.; Cossi, M.; Rega, N.; Millam, J. M.; Klene, M.; Knox, J. E.; Cross, J. B.; Bakken, V.; Adamo, C.; Jaramillo, J.; Gomperts, R.; Stratmann, R. E.; Yazyev, O.; Austin, A. J.; Cammi, R.; Pomelli, C.; Ochterski, J. W.; Martin, R. L.; Morokuma, K.; Zakrzewski, V. G.; Voth, G. A.; Salvador, P.; Dannenberg, J. J.; Dapprich, S.; Daniels, A. D.; Farkas, O.; Foresman, J. B.; Ortiz, J. V.; Cioslowski, J.; Fox, D. J. *Gaussian 09*, Revision A. 02; Gaussian, Inc.: Wallingford, CT, 2009.
(70) Frisch, M. J.; Trucks, G. W.; Schlegel, H. B.; Scuseria, G. E.; Robb, M. A.; Cheeseman, J. R.; Scalmani, G.; Barone, V.; Mennucci, B.; Petersson, G. A.; Nakatsuji, H.; Caricato, M.; Li, X.; Hratchian, H. P.; Izmaylov, A. F.; Bloino, J.; Zheng, G.; Sonnenberg, J. L.; Hada, M.; Ehara, E.; Toyota, K.; Fukuda, R.; Hasegawa, J.; Ishida, M.; Nakajima, T.; Honda, Y.; Kitao, O.; Nakai, H.; Vreven, T.; Montgomery, J. A., Jr.; Peralta, J. E.; Ogliaro, F.; Bearpark, M.; Heyd, J. J.; Brothers, E.; Kudin, K. N.; Staroverov, V. N.; Keith, T.; Kobayashi, R.; Normand, J.; Raghavachari, K.; Rendell, A.; Burant, J. C.; Iyengar, S. S.; Tomasi, J.; Cossi, M.; Rega, N.; Millam, J. M.; Klene, M.; Knox, J. E.; Cross, J. B.; Bakken, V.; Adamo, C.; Jaramillo, J.; Gomperts, R.; Stratmann, R. E.; Yazyev, O.; Austin, A. J.; Cammi, R.; Pomelli, C.; Ochterski, J. W.; Martin, R. L.; Morokuma, K.; Zakrzewski, V. G.; Voth, G. A.; Salvador, P.; Dannenberg, J. J.; Dapprich, S.; Daniels, A. D.; Farkas, O.; Foresman, J. B.; Ortiz, J. V.; Cioslowski, J.; Fox, D. J. *Gaussian 09*, Revision B. 01; Gaussian, Inc.: Wallingford, CT, 2010.
(71) Becke, A. *J. Chem. Phys.* **1993**, *98*, 5648–5652.
(72) Lee, C.; Yang, W.; Parr, R. G. *Phys. Rev. B* **1998**, *37*, 785–789.
(73) Purvis, G. D.; Bartlett, R. J. *J. Chem. Phys.* **1982**, *76*, 1910–1918.
(74) Scuseria, G. E.; Janssen, C. L.; Schaefer, H. F., III. *J. Chem. Phys.* **1988**, *89*, 7382–7387.
(75) Scuseria, G. E.; Schaefer, H. F., III. *J. Chem. Phys.* **1989**, *90*, 3700–3703.
(76) Jacquemin, D.; Wathelet, V.; Perpete, E. A.; Adamo, C. *J. Chem. Theory Comput.* **2009**, *5*, 2420–2435.
(77) Adamo, C.; Barone, V. *J. Chem. Phys.* **1999**, *100*, 6158–6169.
(78) Ernzerhof, M.; Scuseria, G. E. *J. Chem. Phys.* **1999**, *110*, 5029–5036.
(79) Adamo, C.; Barone, V. *J. Chem. Phys.* **1998**, *108*, 664–675.
(80) Zhao, Y.; Truhlar, D. G. *J. Chem. Phys.* **2006**, *125*, No 194101.
(81) Zhao, Y.; Truhlar, D. G. *Theor. Chem. Acc.* **2008**, *120*, 215–241.
(82) Yanai, T.; Tew, D.; Handy, N. *Chem. Phys. Lett.* **2004**, *393*, 51–57.
(83) Chai, J.-D.; Head-Gordon, M. *Phys. Chem. Chem. Phys.* **2008**, *10*, 6615–6620.
(84) Iikura, H.; Tsuneda, T.; Yanai, T.; Hirao, K. *J. Chem. Phys.* **2001**, *115*, 3540–3544.
(85) Tawada, Y.; Tsuneda, T.; Yanagisawa, S.; Yanai, T.; Hirao, K. *J. Chem. Phys.* **2004**, *120*, 8425–8433.
(86) Vydrov, O. A.; Scuseria, G. E. *J. Chem. Phys.* **2006**, *125*, No 234109.
(87) Vydrov, O. A.; Scuseria, G. E.; Perdew, J. P. *J. Chem. Phys.* **2007**, *126*, No 154109.
(88) Srebro, M.; Autschbach *J. Chem. Theory Comput.* **2012**, *8*, 245–256.
(89) Kang, C.-H. Korter, T. M.; Pratt, D. W. *J. Chem. Phys.* **2005**, *122*, No. 174301.
(90) Borin, A. C.; Serrano-Andres *THEOCHEM* **1999**, *464*, 121–128.
(91) Cossi, M.; Scalmani, G.; Rega, N.; Barone, V. *J. Chem. Phys.* **2002**, *117*, 43–54.
(92) Tomasi., J.; Mennucci, B.; Cammi, R. *Chem. Rev.* **2005**, *105*, 2999–3093.
(93) Cossi, R.; Barone, V. *J. Chem. Phys.* **2001**, *115*, 4708–4717.
(94) Grimme, S.; Neese, F. *J. Chem. Phys.* **2007**, *127*, No 154116.
(95) Goerigk, L.; Moellmann, J.; Grimme, S. *Phys. Chem. Chem. Phys.* **2009**, *11*, 4611–4620.
(96) Goerigk, L.; Grimme, S. *J. Chem. Theory Comput.* **2011**, *7*, 3272–3277.
(97) For instance in ref 96, the best performing B2GP-PLYP functional failed to predict the correct order of the ^1L_a and ^1L_b $\pi-\pi^*$ states in one of the PAHs studied, while B2-PLYP failed in four cases.